Eur Radiol (2018) 28:437–445
DOI 10.1007/s00330-017-4989-3

ONCOLOGY

Multi-parametric MRI in cervical cancer: early prediction of response to concurrent chemoradiotherapy in combination with clinical prognostic factors

Wei Yang[1] · Jin Wei Qiang[2] · Hai Ping Tian[3] · Bing Chen[1] · Ai Jun Wang[1] · Jian Guo Zhao[1]

Received: 8 March 2017 / Revised: 9 July 2017 / Accepted: 12 July 2017 / Published online: 4 August 2017

Abstract

Objective To investigate the prediction of response to concurrent chemoradiotherapy (CCRT) through a combination of pretreatment multi-parametric magnetic resonance imaging (MRI) with clinical prognostic factors (CPF) in cervical cancer patients.

Methods Sixty-five patients underwent conventional MRI, diffusion-weighted imaging (DWI), and dynamic contrast-enhanced MRI (DCE-MRI) before CCRT. The patients were divided into non- and residual tumour groups according to post-treatment MRI. Pretreatment MRI parameters and CPF between the two groups were compared and prognostic factors, optimal thresholds, and predictive performance for post-treatment residual tumour occurrence were estimated.

Results The residual group showed a lower maximum slope of increase (MSI_L) and signal enhancement ratio (SER_L) in low-perfusion subregions, a higher apparent diffusion coefficient (ADC) value, and a higher stage than the non-residual tumour group ($p < 0.001$, $p = 0.003$, $p < 0.001$, and $p < 0.001$, respectively). MSI_L and ADC were independent prognostic factors. The combination of both measures improved the diagnostic performance compared with individual MRI parameters. A further combination of these two factors with CPF exhibited the highest predictive performance.

Conclusions Pretreatment MSI_L and ADC were independent prognostic factors for cervical cancer. The predictive capacity of multi-parametric MRI was superior to individual MRI parameters. The combination of multi-parametric MRI with CPF further improved the predictive performance.

Key points

- *Pretreatment MSI_L and ADC were independent prognostic factors for post-treatment residual tumours.*
- *The residual groups showed lower MSI_L, higher ADC and higher stage.*
- *The predictive capacity of multi-parametric MRI was superior to individual MRI parameters.*
- *The combination of multi-parametric MRI with CPF exhibited the highest predictive performance.*

Keywords Magnetic resonance imaging · Dynamic contrast-enhanced MR imaging · Diffusion-weighted imaging · Cervical cancer · Concurrent chemoradiotherapy

Abbreviations

MRI	magnetic resonance imaging
DWI	diffusion-weighted imaging

✉ Jin Wei Qiang
dr.jinweiqiang@163.com

Wei Yang
yangwei_0521@163.com

Hai Ping Tian
happy0951@163.com

Bing Chen
2269415835@qq.com

Ai Jun Wang
1989328313@qq.com

Jian Guo Zhao
fsyszhaojianguo@163.com

[1] Department of Radiology, The General Hospital of Ningxia Medical University, 804 Shengli Road, Yinchuan 750004, China

[2] Department of Radiology, Jinshan Hospital, Fudan University, 1508 Longhang Road, Shanghai 201508, China

[3] Department of Pathology, The General Hospital of Ningxia Medical University, 804 Shengli Road, Yinchuan 750004, China

ADC	apparent diffusion coefficient
DCE-MRI	dynamic contrast-enhanced MRI
MSI	maximum slope of increase
SER	signal enhancement ratio
ROI	region of interest
CPF	clinical prognostic factor

Introduction

Cervical cancer is the fourth most common cancer and remains a leading cause of death worldwide, despite the introduction of effective screening strategies. Approximately 265,700 women die of cervical cancer every year, with 90% of deaths occurring in underdeveloped countries [1]. For patients with advanced cervical cancer, initial concurrent chemoradiotherapy (CCRT) is the most effective treatment and may be the only opportunity to achieve a complete cure. Once initial treatment fails, further treatment options are severely limited [2–4]. Thus, accurate prediction of treatment response as early as possible is critical and may profoundly affect the prognosis of the patient. Clinical prognostic factors (including stage, lymph node status, histology and parametrial invasion) are currently well established to guide therapy selection but do not always translate into successful treatment outcomes because of variations in the prognosis of the disease. Therefore, a reliable early marker of tumour response to therapy must be developed to provide a window of opportunity to modify and improve treatment strategies immediately.

Overcoming morphological limitations of conventional magnetic resonance imaging (MRI), functional MRI is a non-invasive technique and has been more popularly used in clinical practice. Diffusion-weighted imaging (DWI), a common functional imaging modality, can probe water molecule motion in tissue to detect and characterise diseases. Apparent diffusion coefficient (ADC) is a quantitative parameter of DWI and may provide information regarding tumour cellularity and proliferation [5–7]. Studies have reported the potential of DWI in predicting early therapeutic response to CCRT for cervical cancer [8–10]. Dynamic contrast-enhanced MRI (DCE-MRI) has been used to non-invasively assess the microcirculatory perfusion and vascular permeability of the tumour. The maximum slope of increase (MSI) and signal enhancement ratio (SER) are two semi-quantitative parameters that can reflect tumour blood supply and oxygenation status [11], and thereby predict the therapeutic response to anti-angiogenic treatment and CCRT in cervical cancer [12, 13].

This study aimed to evaluate the overall predictive value of response to CCRT through the combination of pretreatment DWI, DCE-MRI biomarkers and pretreatment clinical prognostic factors (tumour stage, pelvic and para-aortic lymph nodes, and histological type) in patients with cervical cancer. A novel predictive paradigm was developed by synergising the predictive capacity of pretreatment clinical prognostic factors and pretreatment multi-parametric MRI.

Materials and methods

Patient Population

The study was approved by the institutional review board and all patients provided a written informed consent. Between December 2014 and January 2016, 74 patients with suspected cervical cancer were prospectively enrolled. They underwent pretreatment multi-parametric MRI, CCRT and MRI follow-up. Inclusion criteria were as follows: (a) uterine cervical cancer confirmed by biopsy, and the time interval between biopsy and baseline MRI no longer than two weeks; (b) tumour maximal diameter > 1.0 cm; (c) no previous radiation or chemotherapy; and (d) no contraindications for CCRT or MRI examination. We excluded three patients with pathologically proven endometrial carcinoma, four patients with a tumour maximal diameter < 1.0 cm and two patients with a history of CCRT for cervical cancers. Finally, 65 patients with uterine cervical cancer were analysed. Based on pretreatment biopsy, they included 59 patients with squamous cell carcinoma, five patients with adenocarcinoma and one patient with adenosquamous carcinoma. The age of the patients ranged from 31 to 75 years with a mean age of 48.3 years. Staging was performed according to the FIGO (International Federation of Gynecology and Obstetrics) staging system [14]. There were three stage I patients, 38 stage II patients, 20 stage III patients and four stage IV patients.

Concurrent chemoradiotherapy (CCRT)

All patients were treated with a combination of external beam radiotherapy (EBRT) and intracavitary brachytherapy (ICR). EBRT was delivered to the entire pelvis at a total dose of 46-50 Gy (1.8-2 Gy dose daily, five times per week), accompanied by concurrent chemotherapy (40 mg/m^2 cisplatin, five cycles weekly). ICR was initiated after an EBRT dose of 46-50 Gy and was delivered twice a week in eight fractional doses of 4 Gy at each point. Overall CCRT for each patient lasted 8 weeks. Based on radical radiotherapy and chemotherapy, each treatment protocol selection was individualised according to tumour extent, lymph node involvement, and general patient condition.

MRI protocol

All patients underwent routine pelvic MRI, DWI, and DCE-MRI before initiating CCRT (pretreatment) and one month after completion of CCRT (post-treatment). MRI was performed using a 3.0 T MRI system (Signa Excite HD, GE,

Milwaukee, WI, USA) with an 8-channel phased array coil. All patients were injected intramuscularly with 20 mg hyoscine butylbromide 10 minutes prior to MR scanning to prevent gastrointestinal motility. The bladder was half-filled to improve lesion visibility. Patients were in the supine position and breathed freely during acquisition. The scanning range was from the aortic bifurcation to the inferior margin of the pubic symphysis. Scanning parameters were as follows: axial fast spin-echo (FSE) T1-weighted images (T1WI) (repetition time [TR]/echo time [TE]: 400 ms/7.3 ms, NEX: 2, slice thickness/gap: 8 mm/1 mm, field of view [FOV]: 380 × 380 mm, acquisition matrix: 384 × 256 mm); axial and sagittal fat suppression (FS) fast spin-echo (FSE) T2-weighted images (T2WI) (TR/TE: 4000 ms/130.2 ms, NEX: 2, slice thickness/gap: 5 mm/1 mm, FOV 380 × 224 mm, acquisition matrix: 240 × 240 mm). Axial DWI was obtained using the echo planer imaging sequence with a diffusion gradient b factor of 0 and 800 s/mm^2 (TR/TE: 2000 ms/56.1 ms, NEX: 4, slice thickness/gap: 8 mm/1 mm, FOV 380 × 342 mm, acquisition matrix: 384 × 342 mm). DCE-MRI was performed using liver acquisition with volume acceleration-extended volume (LAVA-EV) sequence (TR/TE: 6.1 ms/1.1 ms, NEX: 1, slice thickness/gap: 4 mm/-2.0 mm, FOV: 260 × 260 mm; acquisition matrix: 256 × 128 mm) before and immediately after intravenous injection of 0.2 mmol/kg contrast agent (Gd-DTPA, Bayer Schering, Berlin, Germany) at a rate of 2.0 ml/s, then repeated at 30, 60, 90, 120, 150, and 180 s into the examination, followed by a saline flush. The total acquisition time for this sequence was 22-30 s.

Image analysis

All imaging analyses were performed by two radiologists (W.Y. and J.W.Q., with 15 and 32 years of experience in gynaecological imaging, respectively) on a GE ADW 4.4 post-processing workstation with the FUNCTOOL software. Both radiologists were blinded to the clinical and pathological information of the patients. Any discrepancies were resolved by consensus.

An axial slice with the largest solid portion of tumour was selected on DWI by referring to the T2-weighted imaging (T2WI). The regions of interests (ROIs) were drawn manually along the margin of the tumour on this slice, carefully avoiding cystic, necrotic or haemorrhagic tumour regions, and copied to the corresponding ADC map. The average ADC value was automatically generated and recorded as the tumour ADC.

The semi-quantitative parameters were calculated according to the following equation [15]: 1) the maximum slope of increase (MSI) = $(SI_{max} - SI_{pre})/SI_{pre}$; and 2) signal enhancement ratio (SER) = $(SI_{max} - SI_{pre})/(SI_{last} - SI_{pre})$. (SI, signal intensity; SI_{pre}, SI before contrast administration; SI_{max}, maximum SI among enhanced acquisitions; SI_{last}, SI of late acquisitions).

A sagittal section with the largest solid portion of the tumour was selected for acquisition of the time-signal intensity curve (TIC), MSI and SER on DCE-MRI. Because of intratumoural heterogeneous perfusion, approximately 50-70 mm^2 round or round-like ROIs were manually placed both in a low- and high-enhancement subregion separately and were selected based on visual analysis of images according to a previous study [16], carefully avoiding cystic, necrotic or haemorrhagic tumour regions. In cases of small tumours, two different adjacent slices were used to place the two ROIs.

Tumour size was determined by the longest diameter measured in three axes, according to the FIGO staging system [14]. Pelvic and para-aortic lymph nodes were considered positive if they measured > 1.0 cm in the short axis on fat suppression (FS) fast spin-echo (FSE) T2-weighted images.

Pretreatment clinical classification and post-treatment response

Combined clinical prognostic factors were dichotomised into unfavourable (stage III or IV, positive lymph nodes or non-squamous carcinomas) versus favourable (stage I or II, negative lymph nodes and squamous carcinomas) categories. Each clinical prognostic factor was weighted equally.

Treatment response was classified as non-residual and residual tumour groups [17]. All posttherapy MRIs were reviewed by one radiologist (W.Y.) and radiation oncologists in consensus. A non-residual tumour was defined as no tumour found on T2WI and complete disappearance of both the hyperintense tumour area on DWI and the enhanced tumour area on DCE-MRI at one month after completion of the therapy. A residual tumour was defined as a visible residual tumour on T2WI, a hyperintense area on DWI, or an enhanced area on DCE- MRI.

Statistical analysis

Statistical analysis was performed using SPSS 17.0 (SPSS Inc, Chicago, IL, USA). All continuous variables were expressed as the means ± standard deviation (SD) and 95% confidence intervals (CI). A P value less than 0.05 was considered statistically significant. Comparison of MSI, SER, ADC, FIGO stage, lymph nodes status and histological type between non-residual and residual tumour groups was performed using one-way analysis of variance or the Pearson chi-square test, as appropriate. Receiver operating characteristic (ROC) analyses were conducted to determine cut-off values. Diagnostic performances of variables in predicting the occurrence of post-treatment residual tumours were evaluated and compared. Uni- and multivariate logistic regression were used to analyse the prognostic factors.

Results

Pretreatment clinical prognostic factors (CPF: FIGO stage, lymph node status and histological type) and MRI parameters of post-treatment non-residual and residual tumour groups in patients with cervical cancer are shown in Table 1. At one month after CCRT completion, 44 of 65 patients had no residual tumours, and the remaining 21 women had residual tumours on MRI. There was a significantly higher FIGO stage in residual tumours than in non-residual tumours ($p < 0.001$). No significant differences in lymph node status and histological type were found between the two groups ($p = 0.629$ and $p = 0.955$). Lower pretreatment MSI and SER in low-perfusion subregions (0.47 ± 0.33 *vs.* 1.37 ± 0.87, $p < 0.001$; 0.76 ± 0.32 *vs.* 1.02 ± 0.28, $p = 0.003$, respectively) and a significantly higher ADC value (1.10 ± 0.23 *vs.* 0.84 ± 0.11, $p < 0.001$) were found in post-treatment residual tumours than those in non-residual tumours. However, MSI and SER in high-perfusion subregions and tumour size were not significantly different between the two groups ($p = 0.32$, $p = 0.33$, and $p = 0.078$, respectively; Table 1 and Fig. 1).

Univariate logistic regression showed that for pretreatment MSI and SER in low-perfusion subregions, the ADC and FIGO stages were significantly correlated with the occurrence of post-treatment residual tumours. Furthermore, multivariate analysis revealed that only MSI in low-perfusion subregions and ADC were independent prognostic factors. The lower MSI and SER in low-perfusion subregions and higher ADC have higher risk ratios for residual tumour occurrence. As stage increases in disease, pretherapy stage III-IV tumours tended to have a more unfavourable clinical outcome (71%; 17/24 patients) than those in patients with early-stage disease (10%; 4/41 patients; Tables 1 and 2).

ROC curve analysis yielded a cutoff MSI value of 0.62 and SER value of 0.72 in low-perfusion subregions and a cutoff ADC of 0.9×10^{-3}mm^2/s for distinguishing post-treatment residual tumour occurrence from the non-residual tumour. The area under the curve (AUC) of MSI in low-perfusion

Table 1 Comparisons of pretreatment MRI parameters and clinical prognostic factors between post-treatment non-residual and residual tumour groups in patients with cervical cancer

Parameters	Non-residual (n = 44)	Residual (n = 21)	*p* value
MRI parameters			
tumour size (cm)	5.48 ± 1.07 (4.32-6.51)	5.79 ± 1.32 (4.58-7.01)	0.078
MSI_H	1.91 ± 0.24 (0.91-1.51)	1.87 ± 0.56 (0.46-0.83)	0.32
SER_H	1.27 ± 0.43 (0.92-1.05)	1.24 ± 0.89 (0.53-0.85)	0.33
MSI_L	1.37 ± 0.87 (1.10-1.63)	0.47 ± 0.33 (0.33-0.61)	< 0.001
SER_L	1.02 ± 0.28 (0.93-1.10)	0.76 ± 0.32 (0.62-0.93)	0.003
ADC	0.84 ± 0.11 (0.81-0.87)	1.10 ± 0.23 (0.98-1.20)	< 0.001
CPF			
FIGO stage			< 0.001
IB	3	0	
IIA	4	0	
IIB	30	4	
IIIA	1	2	
IIIB	6	11	
IVA	0	2	
IVB	0	2	
Lymph node			0.629
Negative	33	14	
Positive	11	7	
Pelvic LN	10 (8 II, 2 III)	3 (2 III, 1 IV)	
Para-aortic LN	1 (III)	4 (2 III, 2 IV)	
Histology			0.955
Squamous	40	19	
Adenocarcinoma	4 (2 II, 2 IIIB)	1 (IIB)	
Adenosquamous	0	1 (IVA)	

MSI_H: maximum slope of increase (MSI) in high-perfusion subregions; SER_H: signal enhancement ratio (SER) in high-perfusion subregions; MSI_L: MSI in low-perfusion subregions; SER_L: SER in low-perfusion subregions; ADC: apparent diffusion coefficient; CPF: clinical prognostic factors; FIGO: International Federation of Gynecology and Obstetrics; LN: Lymph node. 95% confidence interval (CI) in parentheses

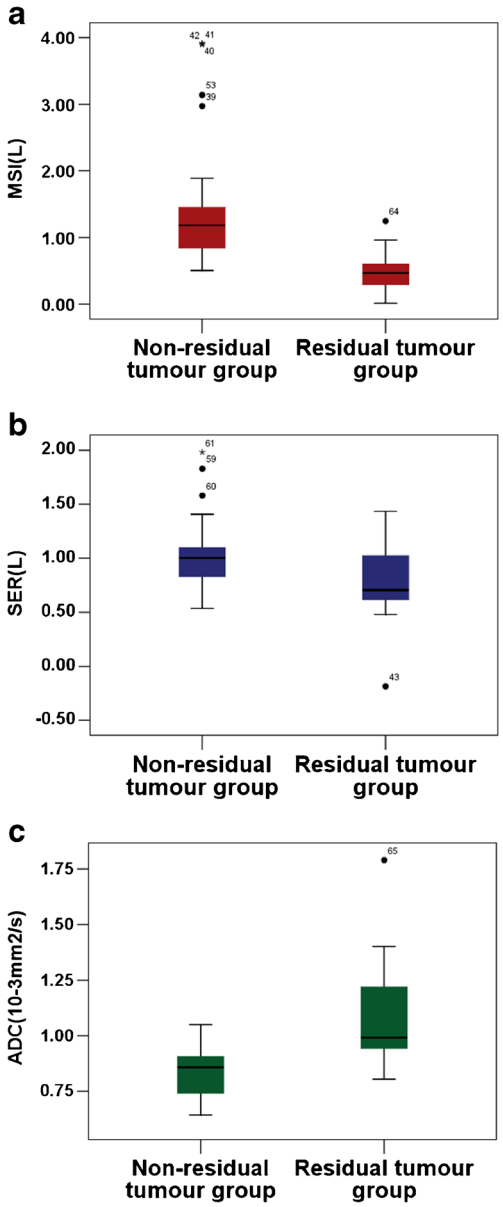

Fig. 1 Box-plot of pretreatment MSI and SER values in low-perfusion subregions and ADC value in non-residual and residual tumour groups

subregions was larger than that of SER (Tables 3, 4, and 5 and Figs. 2, 3 and 4).

Diagnostic performances of MRI, CPF and combined MRI/CPF parameters for predicting post-treatment residual tumour occurrence are shown in Table 3. The sensitivity, specificity and positive and negative predictive values (PPV and NPV) were 95.2%, 76.2%, 89.1% and 84.2%, respectively, for MSI in low-perfusion subregions and 87.5%, 81.8%, 69.2% and 92.3%, respectively, for ADC, in predicting post-treatment residual tumour occurrence. A combination of MSI in the low-perfusion subregions and ADC improved the diagnostic performance with 96.2%, 85.7%, 93.2% and 85.7%, compared with individual MRI parameters alone.

For individual clinical prognostic factors (stage, lymph node status and histological type), sensitivities and specificities were inferior in predicting outcomes. Combined clinical prognostic factors also displayed poor prediction, with a lower sensitivity of 74.7% and lower specificity of 47.6%, compared with multi-parametric MRI.

The combination of multi-parametric MRI and clinical prognostic factors exhibited the highest predictive performance, with a sensitivity of 97.2%, specificity of 93.1%, PPV of 93.2% and NPV of 85.7%, compared with multi-parametric MRI or the combined clinical prognostic factors alone.

Discussion

Because of early occult symptoms, most cervical cancer patients are diagnosed with locally advanced cervical cancer at the time of treatment and are therefore unsuitable for surgical staging [18]. CCRT is often the only possible treatment. Clinical prognostic factors have been deemed suboptimal in predicting outcomes, owing to outcome variability within each prognostic factor [19, 20]. Moreover, given tumour heterogeneity, it is unlikely that all cancers will respond in the same way to a specific therapy [21]. In the present study, multi-parametric MRI was used to reflect different aspects of tumour properties to predict the short-term response to CCRT in cervical cancer and to improve discrimination between non-residual and residual tumours.

The present study showed that a higher ADC value was significantly associated with the occurrence of a residual tumour, which is supported by previous studies [8–10]. Dzik-Jurasz et al. [22] and Patrick et al. [23] explained that an increased ADC value could act as a marker of tumour necrosis, which could be apt to chemoradiotherapy resistance and poor therapy response.

In this study, pretreatment MSI and SER in high-perfusion subregions were not significantly different between the two groups, but MSI and SER in low-perfusion subregions were significantly associated with the presence of a residual tumour, which is supported by a previous study [24]. Mayr et al. [25] also validated that the low-enhanced regions more accurately predicted treatment response within the heterogeneous tumour compared with the high-enhanced regions. Yamashita et al. [16] showed that poorly enhanced areas on dynamic MR images contained fewer capillaries and more abundant fibrous tissues, which are likely to contribute to therapy resistance because the lack of blood supply limits the exposure of the tumour cells to chemotherapy. In addition, low-perfusion subregions could contain hypoxic cells, which are known to possess some radioresistance [26, 27]. Unfortunately, the present study did not examine the histology and molecular markers of these regions, and we only can

Table 2 Univariate and multivariate logistic regression analyses for MRI parameters and CPF in estimating post-treatment residual tumours

Parameters	OR	95% CI	*p*
Univariate analysis			
MRI parameters			
MSI_L	43.73	9.75-193.97	< 0.001
SER_L	24	5.78-∝	< 0.001
ADC	29	6.66-106.99	< 0.001
CPF parameters			
FIGO stage (I-II vs. III-IV)	0.10	0.03-0.33	< 0.001
Lymph node (positive vs. negative)	1.34	0.42-4.25	0.629
Histology (squamous vs. non-squamous)	1.05	0.000-5.45	0.955
Multivariate analysis			
MRI parameters			
MSI_L	36.795	1.574-859.992	0.025
SER_L	0.993	0.030-33.266	0.997
ADC	0.034	0.003-0.454	0.011
CPF parameters			
FIGO stage (I-II vs. III-IV)	3.958	0.519-30.200	0.185

OR: odds ratio; CI: confidence interval; CPF: clinical prognostic factors; MSI_L: MSI in low-perfusion subregions; SER_L: SER in low-perfusion subregions; ADC: apparent diffusion coefficient

Table 3 Diagnostic performance of MRI, CPF and combined MRI/CPF parameters for predicting post-treatment residual tumour occurrence

Parameters	Cutoff value	AUC	*p*	Sensitivity	Specificity	PPV	NPV
MRI							
MSI_L	0.62	0.92	< 0.001	95.2%	76.2%	89.1%	84.2%
SER_L	0.72	0.73	< 0.001	93.5%	57.1%	82.4%	85.7%
ADC	0.90	0.88	< 0.001	87.5%	81.8%	69.2%	92.3%
Combined MRI	—	—	—	96.2%	85.7%	93.2%	85.7%
CPF							
FIGO stage	—	0.81	< 0.001	71.5%	71.4%	84.5%	62.5%
Lymph node	—	0.55	0.57	29.5%	76.2%	72.2%	34.0%
Histological type	—	0.51	0.96	57.1%	9.5%	67.8%	33.3%
Combined CPF	—	—	—	74.7%	47.6%	78.4%	71.4%
Combined MRI-CPF	—	—	—	97.2%	93.1%	93.2%	85.7%

AUC: area under the curve; PPV: positive predictive value; NPV: negative predictive value

Table 4 Multi-parametric MRI for estimating the probability of post-treatment residual tumour occurrence

MRI parameter description		No. of patients	No. of residual tumours	Percentage
Favourable	$MSI_L \geq 0.62$ and $ADC \leq 0.90$	32	1	3%
Intermediate	$MSI_L \geq 0.62$ and $ADC > 0.90$ or $MSI_L < 0.62$ and $ADC \leq 0.90$	18	5	28%
Unfavourable	$MSI_L < 0.62$ and $ADC > 0.90$	15	15	100%

Note: MRI favourable indicates no MRI parameters beyond the threshold; MRI intermediate indicates that one MRI parameter was beyond the threshold; MRI unfavourable indicates that both MRI parameters were beyond the threshold

Table 5 Combined multi-parametric MRI and CPF for estimating the probability of post-treatment residual tumour occurrence

MRI	Favourable CPF			Unfavourable CPF		
	No. of patients	No. of residual tumours	Percentage	No. of patients	No. of residual tumours	Percentage
Favourable	22	0	0%	10	1	10%
Intermediate	6	1	17%	12	4	33%
Unfavourable	2	2	100%	13	13	100%

Note: Favourable CPF: stage I-II, negative lymph node and squamous carcinoma; Unfavourable CPF: stage III-IV or positive lymph node or non-squamous carcinoma

hypothesise about the possible mechanisms leading to residual tumours. Additional studies are necessary to address this issue.

Because of abnormal microvasculature, tumours show a higher signal intensity in DCE-MRI compared with normal tissues. The temporal changes in signal intensity obtained by DCE-MRI imply permeability and perfusion of the tumour microenvironment, both of which profoundly affect therapy outcomes in cervical cancer [28–30]. As one of the DCE-MRI-derived microcirculation variables, MSI is closely related to blood velocity and directly reflects blood flow. SER shows strong correlation with blood volume. Therefore, MSI and SER may be considered effective prognostic indicators to determine the potential efficacy of CCRT [31–33].

Using multi-parametric MRI, the prediction of the therapeutic response to CCRT could be further improved, compared with individual MRI parameters alone. The estimated probability of residual tumour occurrence was almost 100% in patients with both MRI parameters going beyond the thresholds (MSI in low-perfusion subregions < 0.62 and ADC > 0.9×10^{-3}mm^2/s); a residual tumour was present in 28% of patients with one parameter going beyond threshold; and a residual tumour was present in 3% of patients with neither parameter going beyond threshold.

The present study showed that the combination of multi-parametric MRI with clinical prognostic factors (CPF) may create new opportunities for improving prognostic abilities. In patients with unfavourable multi-parametric MRI, despite favourable CPF, the probability of residual tumour occurrence increased from 10% to 100%. In patients with unfavourable CPF and favourable multi-parametric MRI, the probability of residual tumours decreased from 71% to 10%. These results strongly suggest that MRI parameters are superior to CPF in predicting outcomes; MRI parameters play a more important role and CPF is a key complement. The combination of CPF and MRI is a promising tool and offers a window of opportunity to modify initial treatment regimens to improve clinical outcomes. Indeed, early prediction of failure of ongoing standard therapies ought to be implemented with more aggressive treatments, such as radiation dose intensification, changes in concurrent therapy or addition of novel clinical trial therapies. Second, prediction of success may avoid unnecessarily intense or experimental therapies in patients with a low risk of failure, reducing morbidity and healthcare costs.

Our study has several limitations. First, because of the small population of patients, especially those with non-squamous carcinoma, further validation with a larger number

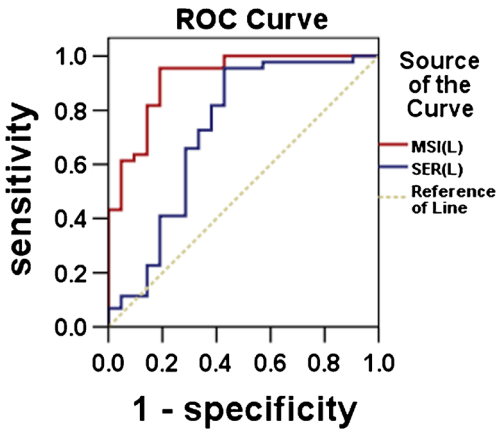

Fig. 2 ROC curves of MSI and SER values in low-perfusion subregions for distinguishing post-treatment residual tumour occurrence from non-residual tumour

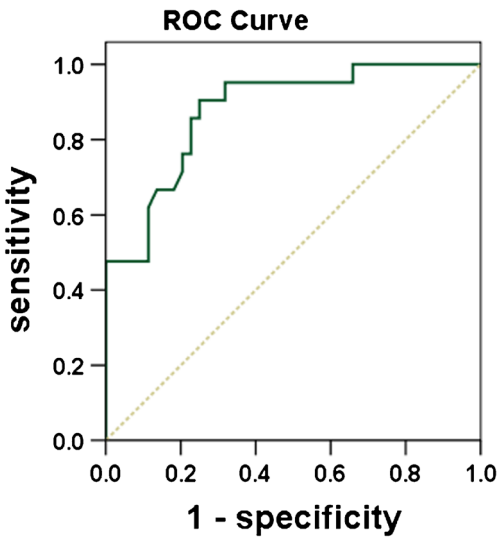

Fig. 3 ROC curve of ADC values for distinguishing post-treatment residual tumour occurrence from non-residual tumour

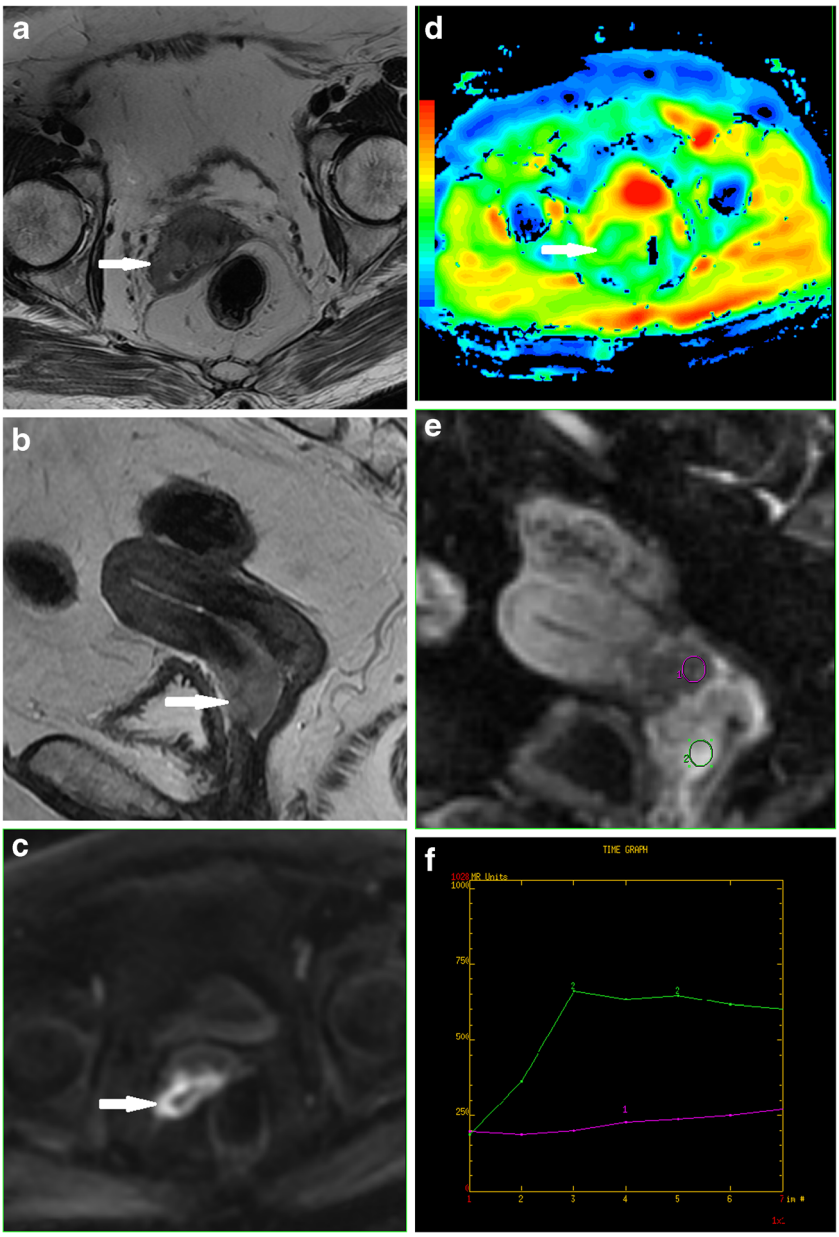

Fig. 4 MR images of a 63-year-old woman with cervical squamous cell carcinoma of stage IIB before concurrent chemoradiotherapy. Axial T1-weighted imaging and sagittal T2-weighted imaging (a and b) show the tumour with an irregular heterogeneous iso- and hyperintensity in the uterine cervix (arrow). Axial diffusion-weighted imaging (c) shows the tumour with an obvious hyperintensity (arrow). Corresponding ADC map (d) shows a decreased ADC value. Sagittal dynamic contrast-enhanced MRI (e) shows the tumour with obviously heterogeneous enhancement. Corresponding time-signal intensity curves (f) of regions of interest (ROIs) show persistent and slow increase in low-perfusion subregions of the tumour (ROI_1) and show a rapid increase and a persistent plateau in high-perfusion subregions (ROI_2)

of patients is necessary. Second, we detected a complete response to CCRT based on post-treatment MRI instead of pathology. It must be emphasised that CCRT-induced changes on imaging can sometimes mimic the presence of a residual tumour. The follow-up period was short and we did not evaluate such clinical endpoints as overall survival rate or progression-free survival. These limitations will have to be addressed in a future study.

In conclusion, MSI in low-perfusion subregions and ADC, both from pretreatment multi-parametric MRI, were independent prognostic factors for post-CCRT residual tumours in patients with cervical cancer. The combination of multi-parametric MRI with pretreatment clinical prognostic factors could significantly improve the predictive performance of the response to CCRT and be a promising tool for the personalised treatment of cervical cancer.

Compliance with ethical standards

Guarantor The scientific guarantor of this publication is Jin Wei Qiang.

Conflict of interest The authors of this manuscript declare no relationships with any companies, whose products or services may be related to the subject matter of the article.

Funding This study has received funding by National Natural Science Foundation of China (No.81471628); Shanghai Municipal Commission

of Health and Family Planning, China (No.2013SY075 and No. ZK2015A05).

Statistics and biometry No complex statistical methods were necessary for this paper.

Ethical approval Institutional Review Board approval was obtained.

Informed consent Written informed consent was obtained from all patients in this study.

Methodology
- prospective
- diagnostic or prognostic study
- performed at one institution.

References

1. Siegel RL, Miller KD, Jemal A (2015) Cancer statistics, 2015. CA Cancer J Clin 65:5–29
2. Chereau E, DE LA Hosseraye C, Ballester M et al (2013) The role of completion surgery after concurrent radiochemotherapy in locally advanced stages IB2-IIB cervical cancer. Anticancer Res 33:1661–1666
3. Leguevaque P, Motton S, Delannes M et al (2011) Completion surgery or not after concurrent chemoradiotherapy for locally advanced cervical cancer? Eur J Obstet Gynecol Reprod Biol 155:188–192
4. Tangjitgamol S, Katanyoo K, Laopaiboon M, Lumbiganon P, Manusirivithaya S, Supawattanabodee B (2014) Adjuvant chemotherapy after concurrent chemoradiation for locally advanced cervical cancer. Cochrane Database Syst Rev 12: (Cd010401)
5. Sun Y, Tong T, Cai S, Bi R, Xin C, Gu Y (2014) Apparent diffusion coefficient (ADC) value:a potential imaging biomarker that reflects the biological features of rectal cancer. Plos One 9, e109371
6. Kuang F, Ren J, Zhong Q, Fu LY, Huan Y, Chen ZQ (2013) The value of apparent diffusion coefficient in the assessment of cervical cancer. Eur Radiol 23:1050–1058
7. Liu Y, Ye ZX, Sun HR, Bai RJ (2015) Clinical application of diffusion-weighted magnetic resonance imaging in uterine cervical cancer. Int J Gynecol Cancer 25:1073–1078
8. Somoye G, Harry V, Semple S et al (2012) Early diffusion weighted magnetic resonance imaging can predict survival in women with locally advanced cancer of the cervix treated with combined chemo-radiation. Eur Radiol 22:2319–2327
9. Kim HS, Kim CK, Park BK, Huh SJ, Kim B (2013) Evaluation of therapeutic response to concurrent chemoradiotherapy in patients with cervical cancer using diffusion-weighted MR imaging. J Magn Reson Imaging 37:187–193
10. Gladwish A, Milosevic M, Fyles A et al (2016) Association of apparent diffusion coefficient with disease recurrence in patients with locally advanced cervical cancer treated with radical chemotherapy and radiation therap. Radiology 279:158–166
11. Harry VN (2010) Novel imaging techniques as response biomarkers in cervical cancer. Gynecol Oncol 116:253–261
12. Kim JH, Kim CK, Park BK, Park SY, Huh SJ, Kim B (2012) Dynamic contrast-enhanced 3-T MR imaging in cervical cancer before and after concurrent chemoradiotherapy. Eur Radiol 22: 2533–2539
13. Loncaster JA, Carrington BM, Sykes JR et al (2002) Prediction of radiotherapy outcome using dynamic contrast enhanced MRI of carcinoma of the cervix. Int J Radiat Oncol Biol Phys 54:759–767
14. Pecorelli S, Zigliani L, Odicino F (2009) Revised FIGO staging for carcinoma of the cervix. Int J Gynaecol Obstet 105:107–108
15. Semple SI, Harry VN, Parkin DE, Gilbert FJ (2009) A combined pharmacokinetic and radiologic assessment of dynamic contrast-enhanced magnetic resonance imaging predicts response to chemoradiation in locally advanced cervical cancer. Int J Radiat Oncol Biol Phys 75:611–617
16. Yamashita Y, Baba T, Baba Y et al (2000) Dynamic contrast-enhanced MR imaging of uterine cervical cancer: pharmacokinetic analysis with histopathologic correlation and its importance in predicting the outcome of radiation therapy. Radiology 216:803–809
17. Nam H, Park W, Huh SJ et al (2007) The prognostic significance of tumor volume regression during radiotherapy and concurrent chemoradiotherapy for cervical cancer using MRI. Gynecol Oncol 107: 320–325
18. Odicino F, Tisi G, Rampinelli F, Miscioscia R, Sartori E, Pecorelli S et al (2007) New development of the FIGO staging system. Gynecol Oncol 107:S8–S9
19. Sevin BU, Lu Y, Bloch DA, Nadjl M, Koechill DR, Averette HE (1996) Surgically defined prognostic parameters in patients with early cervical carcinoma a multivariate survival tree analysis. Cancer 78:1438–1446
20. Takeda N, Sakuragi N, Takeda M et al (2002) Multivariate analysis of histopathologic prognostic factors for invasive cervical cancer treated with radical hysterectomy and systematic retroperitoneal lymphadenectomy. Acta Obstet Gynecol Scand 81:1144–1151
21. Lyng H, Vorren AO, Sundfor K et al (2001) Intra- and intertumor heterogeneity in blood perfusion of human cervical cancer before treatment and after radiotherapy. Int J Cancer 96:182–190
22. Dzik-Jurasz A, Domenig C, George M et al (2002) Diffusion MRI for prediction of response of rectal cancer to chemoradiation. Lancet 360:307–308
23. McVeigh PZ, Syed AM, Milosevic M, Fyles A, Haider MA (2008) Diffusion-weighted MRI in cervical cancer. Eur Radiol 18:1058–1064
24. Huang ZB, Mayr NA, Lo SS et al (2013) Characterizing at-risk voxels by using perfusion magnetic resonance imaging for cervical cancer during radiotherapy. J Cancer Sci Ther 4:254–259
25. Mayr NA, Yuh WTC, Jajoura D et al (2010) Ultra-early predictive assay for treatment failure using functional magnetic resonance imaging and clinical prognostic parameters in cervical cancer. Cancer 116:903–912
26. Kilic S, Cracchiolo B, Gabel M, Haffty B, Mahmoud O (2015) The relevance of molecular biomarkers in cervical cancer patients treated with radiotherapy. Ann Transl Med 18:261
27. Fu Z, Chen D, Cheng H, Wang F (2015) Hypoxia-inducible factor-1alpha protects cervical carcinoma cells from apoptosis induced by radiation via modulation of vascular endothelial growth factor and p53 under hypoxia. Med Sci Monit 21:318–325
28. Zahra MA, Hollingsworth KG, Sala E, Lomas DJ, Tan LT (2007) Dynamic contrast-enhanced MRI as a predictor of tumour response to radiotherapy. Lancet Oncol 8:63–74
29. Mayr NA, Hawighorst H, Yuh WTC, Essig M, Magnotta VA, Knopp MV (1999) MR microcirculation in cervical cancer: correlations with histomorphological tumor markers and clinical outcome. J Magn Reson Imaging 10:267–276
30. Taylor JS, Tofts PS, Port RE et al (1999) MR imaging of tumor microcirculation: promise for the new millennium. J Magn Reson Imaging 10:903–907
31. Li YL, Zhang XP, Li J et al (2015) MRI in diagnosis of pathological complete response in breast cancer patients after neoadjuvant chemotherapy. Eur J Radiol 84:242–249
32. Wu ML, Lu L, Zhang Q et al (2016) Relating doses of contrast agent administered to TIC and semi-quantitative parameters on DCE-MRI: based on a murine breast tumor model. Plos One 11, e0149279
33. Zahra MA, Tan LT, Priest AN et al (2009) Semi-quantitative and quantitative dynamic contrast-enhanced magnetic resonance imaging measurements predict radiation response in cervix cancer. Int J Radiat Oncol Biol Phys 74:766–773